

MIMIX: a Bayesian Mixed-Effects Model for Microbiome Data from Designed Experiments

Neal S. Grantham¹, Yawen Guan¹, Brian J. Reich¹, Elizabeth T. Borer², and Kevin Gross¹

¹Department of Statistics, North Carolina State University, Raleigh, NC

²Department of Ecology, Evolution, and Behavior, University of Minnesota, St. Paul, MN

May 20, 2019

Abstract

Recent advances in bioinformatics have made high-throughput microbiome data widely available, and new statistical tools are required to maximize the information gained from these data. For example, analysis of high-dimensional microbiome data from designed experiments remains an open area in microbiome research. Contemporary analyses work on metrics that summarize collective properties of the microbiome, but such reductions preclude inference on the fine-scale effects of environmental stimuli on individual microbial taxa. Other approaches model the proportions or counts of individual taxa as response variables in mixed models, but these methods fail to account for complex correlation patterns among microbial communities. In this paper, we propose a novel Bayesian mixed-effects model that exploits cross-taxa correlations within the microbiome, a model we call MIMIX (MIcrobiome MIXed model). MIMIX offers global tests for treatment effects, local tests and estimation of treatment effects on individual taxa, quantification of the relative contribution from heterogeneous sources to microbiome variability, and identification of latent ecological subcommunities in the microbiome. MIMIX is tailored to large microbiome experiments using a combination of Bayesian factor analysis to efficiently represent dependence between taxa and Bayesian variable selection methods to achieve sparsity. We demonstrate the model using a simulation experiment and on a 2x2 factorial experiment of the effects of nutrient supplement and herbivore exclusion on the foliar fungal microbiome of *Andropogon gerardii*, a perennial bunchgrass, as part of the global Nutrient Network research initiative.

Keywords: continuous shrinkage prior; factor analysis; microbiome; mixed model; Nutrient Network; OTU abundance data.

1 Introduction

2 A microbiome is a community of microorganisms and their genomes that belong to a particular
3 ecological niche such as the human gut, soil, plants, or ambient dust. Samples collected from
4 these habitats invariably contain thousands of archaea, bacteria, and fungi which may be identified
5 through their DNA with next-generation sequencing technologies (Metzker, 2010). Understanding
6 how these microbial communities interact with their environment holds significant implications for
7 the fields of human health (Wu and Lewis, 2013), climate change (Bond-Lamberty et al., 2016),
8 forensics (Grantham et al., 2015), and more. However, the tools available for characterizing micro-
9 biomes are, at present, largely limited to descriptive studies and must evolve to meet the advanced
10 needs of the microbiome research community. To this end, the interdisciplinary Unified Microbiome
11 Initiative (Alivisatos et al., 2015) aims to achieve “predictive understanding that allows evidence-
12 based, model-informed microbiome management and design” by encouraging collaborative work on
13 several promising areas of emphasis.

14 One such area of emphasis is the development of new statistical models for microbiome data
15 analysis with environmental covariates, particularly in the presence of heterogeneous sources of
16 variability. Microbiome data are difficult to model because they are high-dimensional, sparse, over-
17 dispersed, and possess complex dependence structure. Moreover, as a consequence of the next-
18 generation sequencing technology, the data are compositional, meaning they convey relative rather
19 than absolute information; a microbe’s abundance in a sample (the number of times its DNA was
20 read by the sequencer) depends on the sequencing depth (the total number of reads). Most standard
21 multivariate statistical methods are designed for the analysis of absolute information and will yield
22 spurious correlations among variables when applied indiscriminately to compositional data (Pearson,
23 1896).

24 In the face of these difficulties, contemporary analysis of microbiome data often works on met-
25 rics that summarize collective properties of the entire microbiome, such as measures of taxonomic
26 diversity. For example, in ecology, within-sample diversity is most simply measured as the mean

27 number of unique taxa observed in a sample, referred to as α -diversity. Among-sample diversity,
28 referred to as β -diversity, describes differences in taxonomic composition among samples, and may
29 be quantified by measures like Bray-Curtis dissimilarity (Bray and Curtis, 1957) or, if full taxonomic
30 assignments are available, UniFrac distance (Lozupone and Knight, 2005). Permutational multi-
31 variate analysis of variance (PERMANOVA) with pairwise differences between samples (McArdle
32 and Anderson, 2001) is a popular tool to test whether environmental covariates are associated with
33 significant differences in these summary metrics. However, PERMANOVA does not yield inferences
34 about how the environment affects individual microbes. Additionally, implicit assumptions made by
35 such distance-based multivariate methods may be inappropriate for ecological count data altogether
36 (Warton et al., 2012).

37 More recently, and in a different vein, others have suggested analyzing the microbiome by fitting a
38 separate generalized linear mixed model to the abundance of each taxon. For instance, a linear mixed
39 model with arcsine square root transformation or, if sparsity and overdispersion are of particular
40 concern, a zero-inflated beta model (E. Chen and Li, 2016) are viable methods for inferring treatment
41 effects on the relative abundance (proportions) of taxa in the presence of random effects. Alternative
42 approaches model the raw abundance (counts) directly, accounting for the uncertainty associated
43 with a taxon’s abundance by conditioning on the total reads per sample (McMurdie and Holmes,
44 2014). Hierarchical mixtures, such as beta-binomial and gamma-Poisson, are quite robust for this
45 purpose and possess added flexibility for overdispersed data (Zhang et al., 2017).

46 An alternative to these univariate approaches is to model taxa within the microbiome jointly
47 rather than individually. Unlike univariate models, multivariate models can pool information across
48 taxa to increase power for detecting and estimating treatment effects. Towards this end, the
49 Dirichlet-multinomial (DM) model — the multivariate extension of beta-binomial — provides a
50 rich framework for modeling the entire vector of raw abundance data in each microbiome sample.
51 For example, the DM has proven useful for microbiome analysis in the areas of hypothesis testing
52 and power calculations (La Rosa et al., 2012), sparse variable selection (J. Chen and Li, 2013), infer-
53 ence of microbial community structure (Shafiei et al., 2015), and regression modeling (Wadsworth

54 et al., 2017). Despite their utility, without further hierarchical structure Dirichlet variates have
55 the undesirable property that they must negatively co-vary, making them ill-suited for modeling
56 microbial taxa that often have positive associations, perhaps because they share similar habitat
57 niches or because they interact symbiotically.

58 Models with more flexible dependence structures among microbial taxa have recently been pro-
59 vided by Xia et al. (2013) and Ren et al. (2017). Xia et al. (2013) use a logistic normal multinomial
60 (LNM) model that links the multinomial probability vector to a multivariate normal random vari-
61 able, resulting in unconstrained occurrence probabilities on the linked scale. The covariance struc-
62 ture specified by Xia et al. (2013) captures both positive and negative associations among taxa,
63 unlike the DM covariance. However, while suitable for small collections of taxa, their method for
64 estimating this dependence structure is infeasible for high numbers of unique taxa produced by next-
65 generation sequencing technologies. In a different vein, Ren et al. (2017) use dependent Dirichlet
66 processes to develop a Bayesian nonparametric ordination that enables convenient visualization of
67 differences among microbial communities. Mixed-model versions of any of these approaches — DM,
68 LNM, or Bayesian nonparametric ordination — needed to analyze experiments following split-block
69 designs have yet to be developed for microbiome data, owing to the difficulty of introducing random
70 effects into the model hierarchy.

71 With these considerations in mind, we propose MIMIX (MIcrobiome MIXed model), a Bayesian
72 mixed-effects model for analyzing microbiome data as a response variable in designed experiments.
73 MIMIX achieves four scientific objectives: (1) global tests of whether experimental treatments affect
74 microbiome composition; (2) local tests for treatment effects on individual taxa and estimation of
75 such effects if present; (3) quantification of how different sources of variability contribute to the
76 microbiome heterogeneity; and (4) characterization of latent structure in the microbiome, which
77 may suggest ecological subcommunities. MIMIX is a LNM mixed model that uses Bayesian factor
78 analysis (Rowe, 2002) to capture complex dependence patterns among microbial taxa. Specifically,
79 MIMIX models high-dimensional relationships among the transformed abundance probabilities of
80 individual taxa through a set of low-dimensional unobservable variables, or factors. MIMIX natu-

81 rally identifies clusters of microbes that respond similarly to experimental conditions by developing
82 continuous shrinkage Dirichlet-Laplace priors (Bhattacharya et al., 2015) for these latent factors.
83 We then apply Bayesian variable selection priors for the fixed effects on subpopulation abundance,
84 reflecting the prior belief that treatments will not affect all ecological communities. In this paper,
85 these objectives and features of MIMIX are motivated by a multi-location randomized complete
86 block design (RCBD) experiment that seeks to identify the influence of nutrient supplement and
87 herbivory on the foliar fungal microbiome of a common perennial prairie bunchgrass.

88 The paper proceeds as follows. Section 2 introduces the data that motivate our development
89 of MIMIX in Section 3. Section 4 demonstrates our method on simulated data in comparison with
90 competing microbiome data analysis methods. Finally, we apply MIMIX to RCBD experiment data
91 in Section 5 and close with a discussion in Section 6. Details of posterior sampling schemes are left
92 to the Appendix, and open-source code to reproduce the statistical analyses in this paper is available
93 online at <https://www.github.com/nsgrantham/mimix>.

94 2 Motivating Data

95 The Nutrient Network (NutNet, www.nutnet.org) is a global research cooperative hosted at the
96 University of Minnesota that uses a standardized experimental protocol to study the impact of
97 human activity at over 100 grassland sites spanning 6 continents (Borer et al., 2014). This article
98 is motivated by data collected at 4 of these sites, all in the central US (Iowa, Kansas, Kentucky,
99 and Minnesota). Each of these 4 sites features a 2×2 factorial experiment that crosses a nutrient-
100 supplement treatment (i.e., fertilization) with an herbivore-exclusion treatment in a randomized
101 complete block design (RCBD) (Figure 1). Here, we consider the effect of the two experimental
102 treatments on the foliar fungal microbiome of *Andropogon gerardii*, a perennial bunchgrass found
103 at each site, and native to prairie ecosystems of central North America.

104 In August 2014, leaf samples were collected from four *A. gerardii* individuals in each treatment
105 plot. Samples were collected from plots in three replicated blocks, except in Iowa where *A. gerardii*

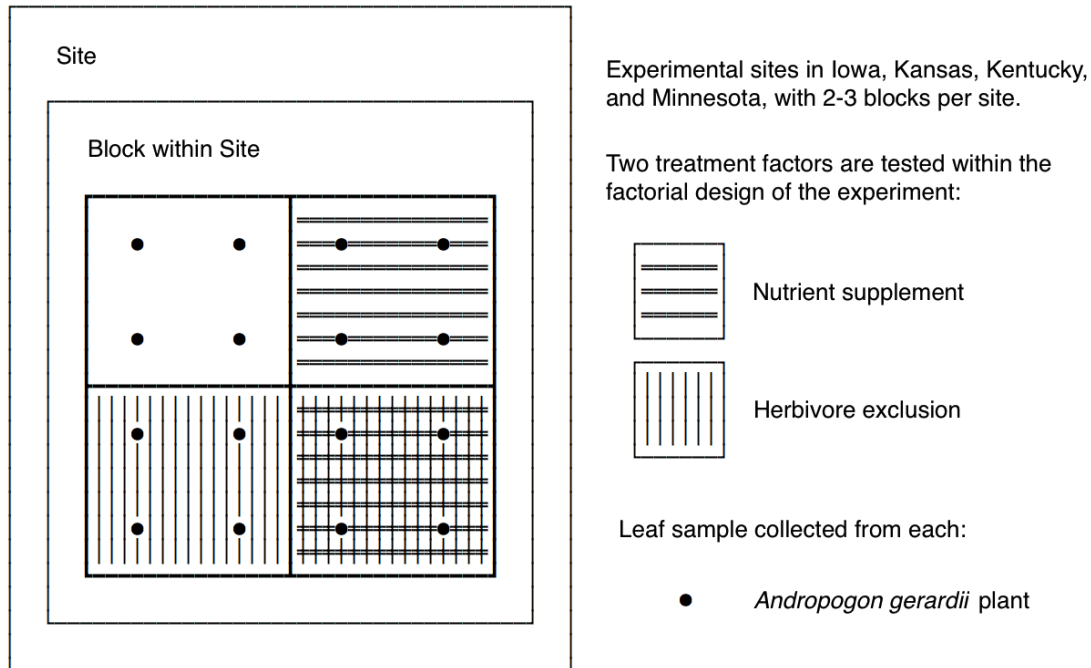


Figure 1: A schematic representation of the Nutrient Network experimental design. This experiment replicates a 2x2 RCB design across several sites. Four plants are sampled from each plot and a microbial sample is collected from each plant late in the growing season.

106 was present in only two blocks. Fungal rDNA was amplified and sequenced from each sample, and
 107 counts of operational taxonomic units (OTUs) within each sample were recorded. (Details of the
 108 molecular methods and bioinformatics pipeline are provided in the Supplement.) Ten samples were
 109 later removed from the study due to errors during sequencing, leaving a total of 166 leaf samples.
 110 Overall, 2,662 fungal OTUs were identified across the 166 samples. Samples contained a median of
 111 74,099 separate reads, and harbored an average of 200 unique OTUs. Many OTUs were rare, as
 112 85% of OTUs were identified in <10% of samples.

113 Given the preliminary OTU assignments, we wish to investigate each of the following using these
 114 data. First, we seek to characterize how the experimental treatments affect microbiome communi-
 115 ties. We perform this analysis in stages: first at a global level where the response is the composition
 116 of the microbiome community as a whole, and then (if the global test identifies a significant treat-
 117 ment effect) at a local level that characterizes the effects on the relative abundance of individual
 118 OTUs. Second, we wish to characterize how the residual variation in the microbiome composition

119 varies among blocks within sites and across sites, as quantifying these sources of variation may
 120 suggest insight into the ecological processes controlling these microbial communities. Finally, we
 121 wish to characterize the dependence structure among OTUs, and identify clusters of OTUs that
 122 may suggest underlying ecological subcommunities.

123 3 Methods

124 Let Y_{ik} denote the count for sample $i = 1, \dots, n$ and taxon $k = 1, \dots, K$, and let $m_i = \sum_{k=1}^K Y_{ik}$
 125 be the total counts for sample i . The value of m_i is an artifact of the sequencing depth of the
 126 high-throughput sequencing process and thus analyses are performed conditional on its value. For
 127 observation i , let \mathbf{x}_i be a p -vector of covariates and let $z_i \in \{1, \dots, q\}$ record the source of the random
 128 effects from one of q blocking factors. This latter notation may be generalized to accommodate
 129 arbitrarily complex blocking designs, but for notational simplicity we assume a single blocking
 130 factor in this initial development.

131 A multinomial likelihood is natural for multivariate count data, so we take $\mathbf{Y}_i = (Y_{i1}, \dots, Y_{iK})' \sim$
 132 $\text{Multinomial}(m_i, \boldsymbol{\phi}_i)$ where $\boldsymbol{\phi}_i = (\phi_{i1}, \dots, \phi_{iK})'$ is the vector of expected proportions with $\boldsymbol{\phi}_i \in$
 133 $\mathbb{S}^K = \{(\phi_1, \dots, \phi_K)' : \phi_k \geq 0, k = 1, \dots, K, \sum_{k=1}^K \phi_k = 1\}$. We define sample-specific $\boldsymbol{\theta}_i =$
 134 $(\theta_{i1}, \dots, \theta_{iK})' \in \mathbb{R}^K$ mapped to \mathbb{S}^K by the inverse log-ratio transformation (Aitchison, 1986)

$$135 \quad \phi_{ik} = \phi_k(\boldsymbol{\theta}_i) = \frac{\exp(\theta_{ik})}{\sum_{l=1}^K \exp(\theta_{il})} \quad \text{for } k = 1, \dots, K. \quad (1)$$

136 There is a loss of dimension in transforming from \mathbb{R}^K to \mathbb{S}^K due to the latter's unit-sum constraint.
 137 The likelihood is invariant to adding a constant to the parameters θ_{ik} ; however, as the prior mean
 138 of the average $\sum_k \theta_{ik}$ is 0, the parameters will tend to be centered around 0 in the posterior.

139 In the spirit of Billheimer et al. (2001), we associate fixed and random effects with the microbiome
 140 composition through the mean of $\boldsymbol{\theta}_i$. The mixed effects decomposition is given by $\boldsymbol{\theta}_i = \boldsymbol{\mu} + \boldsymbol{\beta}\mathbf{x}_i +$
 141 $\boldsymbol{\gamma}_{z_i} + \boldsymbol{\epsilon}_i$, where $\boldsymbol{\mu} = (\mu_1, \dots, \mu_K)'$ is the overall population mean, $\boldsymbol{\beta}$ is a $K \times p$ matrix of unknown

142 fixed effect coefficients, γ_r is a K -vector of random effects from block r , and $\epsilon_i \stackrel{iid}{\sim} N_K(\mathbf{0}, \mathbf{\Omega})$ is
 143 sample-specific random variation. Conditioned on the random effects, the regression coefficient
 144 for covariate j and taxon k , β_{jk} , has the usual logistic regression interpretation when reducing
 145 compositional data to the binary outcome that a sample comes from taxon k versus any of the
 146 other $K - 1$ taxa. That is, with all else fixed, if the j^{th} covariate increases by one the log odds of a
 147 sample coming from taxon k increase by β_{jk} .

148 The number of taxa, K , is often very large in microbiome compositions. To address compli-
 149 cations due to high dimensionality and to account for relationships among taxa, we use Bayesian
 150 factor analysis (Rowe, 2002) to model the fixed and random effects within a lower dimensional
 151 representation. For a number of factors L , let $\mathbf{\Lambda} = (\boldsymbol{\lambda}_1, \dots, \boldsymbol{\lambda}_L)$ be the $K \times L$ latent factor loading
 152 matrix, unknown and to be estimated. Suppose $\mathbf{\Lambda}$ is common to all fixed and random components
 153 of the model, i.e., $\boldsymbol{\beta} = \mathbf{\Lambda}\mathbf{b}$, $\boldsymbol{\gamma}_r = \mathbf{\Lambda}\mathbf{g}_r$, $r = 1, \dots, q$, and $\boldsymbol{\epsilon}_i = \mathbf{\Lambda}\mathbf{e}_i + \boldsymbol{\delta}_i$, $i = 1, \dots, n$. Then we may
 154 represent $\boldsymbol{\theta}_i = \boldsymbol{\mu} + \mathbf{\Lambda}\mathbf{f}_i + \boldsymbol{\delta}_i$ where $\mathbf{f}_i = \mathbf{b}\mathbf{x}_i + \mathbf{g}_{z_i} + \mathbf{e}_i$ is the low-dimensional factor score vector for
 155 sample i . Under this common factor structure each latent factor captures sets of taxa correlated
 156 in their response to the model’s covariates and other sources of variability. This shared-factor as-
 157 sumption is not inherent to our approach and if separate factors are thought to drive the fixed and
 158 random effects then these two components can be modelled separately.

159 A prior on $\mathbf{\Lambda}$ should ensure that the factor loading matrix captures common, cross-species co-
 160 variance that lends itself to post-hoc inference of collective taxa responses. For instance, setting
 161 entire columns of $\mathbf{\Lambda}$ to zero is a means of selecting the number of active factors and setting individual
 162 elements within $\mathbf{\Lambda}$ to zero allows the factors to represent subsets of taxa (Carvalho et al., 2008). To
 163 achieve both forms of sparsity, we place continuous shrinkage priors on the high-dimensional factor
 164 loadings $\boldsymbol{\lambda}_l, l = 1, \dots, L$ comprising $\mathbf{\Lambda}$. In particular, we select a Dirichlet-Laplace prior (Bhat-
 165 tacharya et al., 2015) for its ability to detect sparse signals in high-dimensional linear regression,
 166 which we modify here for factor analysis. For factors $l = 1, \dots, L$, let $\boldsymbol{\lambda}_l \sim \text{DL}_{a_l}$ represented by

167
$$\lambda_{kl} \mid \xi_{kl}, \tau_l \sim \text{Lap}(\xi_{kl}\tau_l), \boldsymbol{\xi}_l = (\xi_{1l}, \dots, \xi_{Kl})' \sim \text{Dir}(a_l, \dots, a_l), \text{ and } \tau_l \sim \text{Gam}(Ka_l, \nu)$$

168 for $k = 1, \dots, K$, where $\nu \sim \mathcal{G}(c_0, d_0)$ and each a_l is given a discrete uniform prior over $(0, 1)$ with
 169 smaller values favoring aggressive shrinkage of terms toward zero. The Laplace distribution may be
 170 equivalently represented as a scale mixture of normals with exponential mixing density,

$$171 \quad \lambda_{kl} \mid \psi_{kl}, \xi_{kl}, \tau_l \sim N(0, \psi_{kl} \xi_{kl}^2 \tau_l^2) \quad \text{and} \quad \psi_{kl} \sim \text{Exp}(1/2),$$

172 a form that allows for straightforward Gibbs sampling of the associated parameters.

173 Another aim of this model is to test and quantify treatment effects on each taxon, so we place a
 174 spike-and-slab prior on \mathbf{b} for the purposes of stochastic variable selection (Mitchell and Beauchamp,
 175 1988). Unlike the DL prior, the spike-and-slab prior places probability on the coefficients being
 176 exactly zero. This allows us to compute posterior probabilities that effects are zero leading to a
 177 Bayesian test, satisfying one of MIMIX's objectives. Let ω_{jl} be an indicator variable taking the
 178 value 1 (0) when b_{jl} is included (excluded) from the model. The spike-and-slab prior is given
 179 by $Pr(\omega_{jl} = 0) = 1 - \pi_j$ and $b_{jl} \mid \omega_{jl} = 1 \sim N(0, \sigma_b^2)$, where $\pi_j \sim \text{Beta}(a_0, b_0)$ is the inclusion
 180 probability for covariate j in the model. We select a_0 and b_0 such that the prior inclusion probability
 181 for each covariate is set at some $c \in [0, 1]$. In particular, the number of factors for which fixed effect
 182 j is active, $S_j = \sum_{l=1}^L \omega_{jl}$, follows a beta-binomial distribution such that $Pr(S_j > 0) = 1 - Pr(S_j =$
 183 $0) = 1 - \frac{\Gamma(L+b_0)\Gamma(a_0+b_0)}{\Gamma(L+a_0+b_0)\Gamma(b_0)}$, where $\Gamma(\cdot)$ is the gamma function. Fixing this quantity at c and selecting
 184 $a_0 = 1$ for convenience, we use the property that $\Gamma(n+1) = n\Gamma(n)$ for any positive integer n to
 185 arrive at $b_0 = (\frac{1-c}{c})L$.

186 Placing priors on the remaining parameters and hyperparameters of this model completes the
 187 Bayesian specification. We use continuous priors for the intercept and random effects terms as we do
 188 not intend to test whether or not they are zero. Let $\mu_k \stackrel{iid}{\sim} N(0, \sigma_\mu^2)$, $g_{rl} \stackrel{iid}{\sim} N(0, \sigma_g^2)$, $e_{il} \stackrel{iid}{\sim} N(0, \sigma_e^2)$
 189 where $\sigma_e^2 = 1$ to identify the scale of \mathbf{A} , and $\delta_{ik} \stackrel{iid}{\sim} N(0, \sigma_k^2)$ where σ_k^2 can capture over-dispersion

190 in the sequence reads of taxon k . These choices induce covariance

$$191 \quad Cov(\boldsymbol{\theta}_i, \boldsymbol{\theta}_{i'} | \boldsymbol{\mu}, \mathbf{b}, \boldsymbol{\Lambda}, \boldsymbol{\Sigma}, \sigma_g) = \begin{cases} (\sigma_g^2 + 1)\boldsymbol{\Lambda}\boldsymbol{\Lambda}' + \boldsymbol{\Sigma} & i = i' \\ \sigma_g^2\boldsymbol{\Lambda}\boldsymbol{\Lambda}' & i \neq i' \text{ and } z_i = z_{i'} \\ \mathbf{0} & z_i \neq z_{i'} \end{cases}$$

192 where $\boldsymbol{\Sigma}$ is the $K \times K$ diagonal matrix with diagonal elements $(\sigma_1^2, \dots, \sigma_K^2)$. The expression of the
 193 covariance of $\boldsymbol{\theta}_i$ illustrates that the product $\boldsymbol{\Lambda}\boldsymbol{\Lambda}'$ but not the individual elements of $\boldsymbol{\Lambda}$ are identified;
 194 we therefore use the posterior of $\boldsymbol{\Lambda}\boldsymbol{\Lambda}'$ to summarize the posterior of the covariance structure. We
 195 suppose the variance terms of the model follow independent inverse gamma priors with shape u_0 and
 196 scale v_0 . The most important tuning parameters are the inclusion probability, c , and the number
 197 of latent factors, L . We set $c = 0.5$ so that each hypothesis has the same prior probability which is
 198 reasonable in our studies with a small number of fixed effects. The number of latent factors, L , is
 199 set to the minimum of the number of samples and the number of taxa (i.e., the maximum number
 200 of identifiable factors) and allows the Dirichlet-Laplace shrinkage prior to eliminate unnecessary
 201 factors.

202 Posterior sampling is conducted using Markov chain Monte Carlo (MCMC). Most terms in this
 203 model formulation are conjugate and are updated via Gibbs sampling. One exception is $\boldsymbol{\theta}_i$ which
 204 we update with Hamiltonian Monte Carlo (HMC) (Neal et al., 2011). The details of these sampling
 205 schemes are found in the Online Supplement. Code to perform MCMC is written in Julia (Bezanson
 206 et al., 2017) and available online at <https://www.github.com/nsgrantham/mimix>.

207 4 Simulation Study

208 We test our model on a simulated experiment with $K = 100$ taxa, $p = 1$ fixed effect, one blocking
 209 factor that takes $q = 5$ levels, and $n = 40$ observations with 8 assigned to each block. Within each
 210 block exists a balanced experiment with two levels of a single experimental factor, where $x_i = 1$

211 if observation i receives one level of the experimental factor, and $x_i = 0$ otherwise, and $z_i = r$ if
212 observation i belongs to block r .

213 The fixed treatment effect, β , is a sparse K -vector with a varying percentage of non-zero ele-
214 ments: 0% dense ($\beta = \mathbf{0}$, i.e., no signal), 10% dense, or 20% dense. To generate β that is 10%
215 dense, we partition the taxa into 20 clusters of 5 taxa each, select two of the twenty groups at
216 random, and within each group draw a value from $v \sim \text{Unif}([-3, -1] \cup (1, 3])$ to signify the group's
217 collective response to the fixed treatment. That is, $\beta_k = v$ if taxon k belongs to the selected group
218 and $\beta_k = 0$ otherwise. For 20% dense, we do this for four total groups. These groups are designed
219 to represent taxa with shared phylogenetic ancestry or taxa that react similarly to the fixed effect.
220 In the Online Supplement, we also investigate a scenario in which OTUs respond to the treatment
221 individually, instead of in groups.

222 For the random blocking effects, we draw $\gamma_r \stackrel{iid}{\sim} N_K(\mathbf{0}, \Sigma_\gamma)$ with autoregressive covariance
223 $(\Sigma_\gamma)_{kk'} = \sigma_\gamma^2 \rho_\gamma^{|k-k'|}$, $\rho_\gamma = 0.9$. Block-to-block variability, σ_γ^2 , is set at 1 (medium) or 4 (high).
224 For each observation i , define $\theta_i = \mu + \beta x_i + \gamma_{z_i} + \epsilon_i$, where μ is a vector of length K with equally-
225 spaced steps from 1 to -1 and $\epsilon_i \stackrel{iid}{\sim} N_K(\mathbf{0}, \Sigma_\epsilon)$ with autoregressive covariance $(\Sigma_\epsilon)_{kk'} = \sigma_\epsilon^2 \rho_\epsilon^{|k-k'|}$.
226 We fix $\rho_\epsilon = 0.9$ and examine sample-to-sample variability, σ_ϵ^2 , over 1 (medium), 4 (high), and 9 (very
227 high). Finally, we arrive at the final data by drawing each vector of counts \mathbf{Y}_i from a multinomial
228 distribution with total counts m_i chosen at-random from 2,500 to 5,000 and taxa proportions ϕ_i
229 calculated according to (1). We do not generate data directly from the MIMIX model to test for ro-
230 bustness to model assumptions (e.g., fixed and random effect correlation); data generated assuming
231 a low-dimensional dependence structure would unduly favor MIMIX over the competitors.

232 In total, we examine each of 18 factor combinations (0, 10, and 20 % dense, medium/high block
233 variance, medium/high/very high error variance) with 50 replications and compare the performance
234 of three competing microbiome data analysis methods:

- 235 1. **PERMANOVA**: Permutational multivariate analysis of variance (McArdle and Anderson,
236 2001), or PERMANOVA, with Bray-Curtis dissimilarity (BC), a common analysis procedure

237 in ecology. This method tests the null hypothesis that there is no difference between the
238 centroids of the treatment and control groups in BC space, but is unequipped to perform
239 parameter estimation. It is implemented by `adonis` in the R package `vegan` 2.3-5 R, among
240 other available software options.

241 2. **MIMIX**: Our Bayesian mixed-effects model as presented in Section 3 with $L = 40$ factors.
242 10,000 posterior samples are collected with 5,000 removed for burn-in.

243 3. **MIMIX w/o Factors**: Bayesian mixed-effects model with no factors. This formulation
244 mimics the available mixed model approaches to microbiome data analysis that do not account
245 for dependence patterns among taxa, i.e., $\mathbf{\Lambda} = \mathbf{I}_K$ and $\mathbf{e}_i = \mathbf{0}$ for all $i = 1, \dots, n$. 10,000
246 posterior samples are collected with 5,000 removed for burn-in.

247 Additional simulation results are given in the Online Supplement.

248 The methods are first evaluated on their power/type I error of a global test for treatment effect
249 where PERMANOVA rejects for p -value < 0.05 and MIMIX and MIMIX w/o Factors reject if
250 $Pr(\boldsymbol{\beta} \neq \mathbf{0} \mid \mathbf{Y}) > 0.9$. We reject if $Pr(\boldsymbol{\beta} \neq \mathbf{0} \mid \mathbf{Y}) > 0.9$ to construct a test that has roughly the
251 same size as the PERMANOVA test. Adopting this rule, both MIMIX and MIMIX w/o Factors
252 regularly outperform PERMANOVA in detecting the presence of a significant signal (Figure 2).
253 In situations with medium error variance, MIMIX and MIMIX w/o Factors achieve similar power
254 regardless of the block variance. As error variance increases, MIMIX is more likely than MIMIX
255 w/o Factors to correctly identify the presence of a significant treatment effect.

256 We further compare MIMIX and MIMIX w/o Factors on their local tests and estimation of
257 treatment effects for each OTU. Several metrics are considered: root mean squared error, $RMSE =$
258 $\sqrt{\frac{1}{K} \sum_{k=1}^K (\hat{\beta}_k^{\text{mean}} - \beta_k)^2}$ where $\hat{\beta}_k^{\text{mean}}$ is the posterior mean of β_k , coverage of 95% credible intervals,
259 $C95 = \frac{1}{K} \sum_{k=1}^K I(\hat{\beta}_k^{0.025} < \beta_k < \hat{\beta}_k^{0.975})$ where $\hat{\beta}_k^q$ is the posterior q th quantile of β_k , and the true
260 positive rate (TPR) and true negative rate (TNR) of local tests that reject if the 95% credible
261 interval for β_k excludes zero. Table 1 gives the values of these metrics averaged over 50 replications
262 at each factor combination.

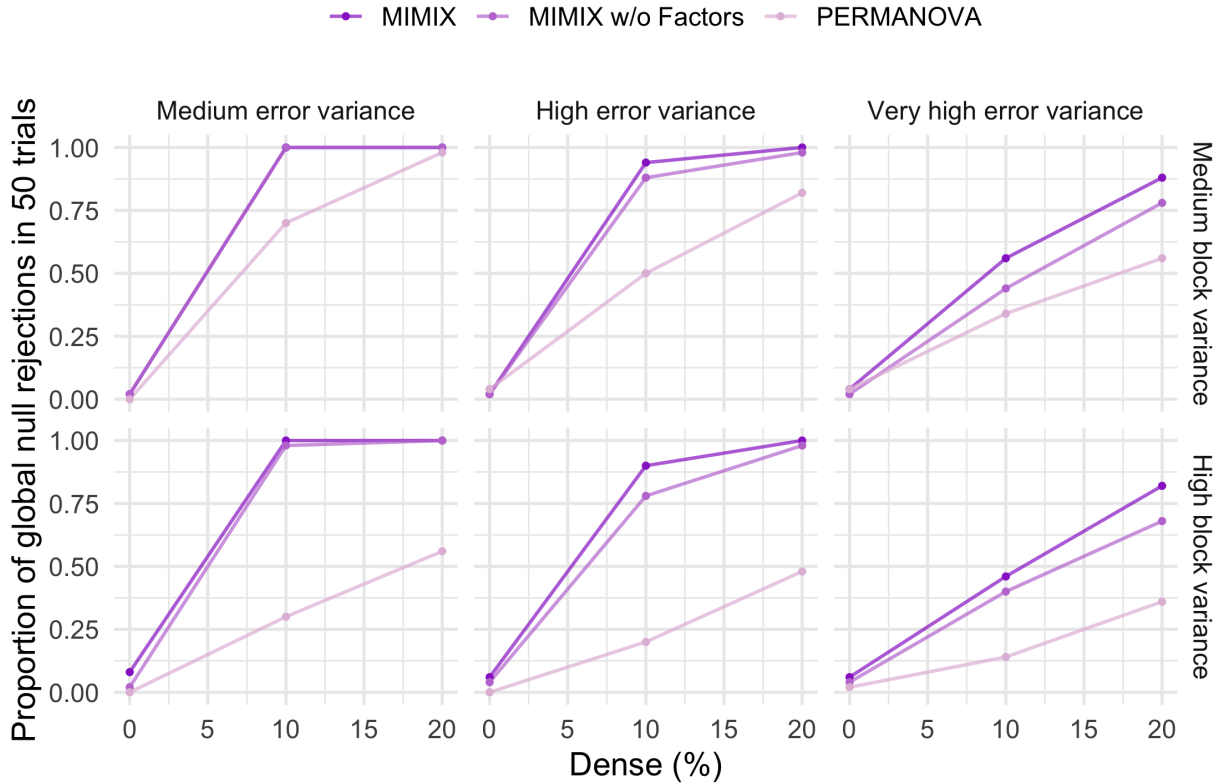


Figure 2: Results of a global test for treatment effect by MIMIX, MIMIX w/o Factors, and PERMANOVA, under a variety of simulation conditions. When $\beta = \mathbf{0}$ (0% Dense) the line gives the test's type I error. For $\beta \neq \mathbf{0}$ (>0% Dense), the line values depict the statistical power of each test.

263 When there is no signal present in the fixed effects (i.e., $\beta = \mathbf{0}$, or 0% dense), MIMIX w/o
 264 Factors achieves lower RMSE on average than MIMIX in estimating all treatment effects to be zero,
 265 and both methods yield credible intervals that nearly always correctly include zero. In practice,
 266 these estimates are inconsequential if the global test appropriately fails to identify a significant
 267 treatment effect. When a proportion of OTUs are affected by the treatment (10% dense and 20%
 268 dense), MIMIX regularly outperforms MIMIX w/o Factors in the detection and estimation of these
 269 non-zero fixed effects. Specifically, when error variance is medium, the TPR of MIMIX is very high
 270 (85.7% to 94.0%) and beats MIMIX w/o Factors (68.6% to 79.5%), whereas the RMSE of the two
 271 methods are comparable. For high error variance, the TPR drops to about 50% (MIMIX) and 20%
 272 (MIMIX w/o Factors), with higher RMSE achieved by both methods, as expected, but lower RMSE
 273 obtained by MIMIX on average. This trend continues with very high error variance, resulting in

Table 1: Local test and estimation performance for MIMIX and MIMIX w/o Factors under a variety of simulation conditions as measured by root mean squared error (RMSE), coverage of 95% credible intervals (C95), true positive rate (TPR), and true negative rate (TNR). All values are multiplied by 100.

| Dense | Error var. | Method | Medium block variance | | | | High block variance | | | |
|-------|------------|-------------|-----------------------|-------|------|-------|---------------------|-------|------|-------|
| | | | RMSE | C95 | TPR | TNR | RMSE | C95 | TPR | TNR |
| 0% | Medium | MIMIX | 0.3 | 100.0 | | 100.0 | 0.6 | 99.6 | | 99.6 |
| | | w/o Factors | 0.0 | 100.0 | | 100.0 | 0.1 | 100.0 | | 100.0 |
| | High | MIMIX | 0.9 | 100.0 | | 100.0 | 1.9 | 99.9 | | 99.9 |
| | | w/o Factors | 0.1 | 100.0 | | 100.0 | 0.5 | 100.0 | | 100.0 |
| | Very High | MIMIX | 2.0 | 100.0 | | 100.0 | 3.3 | 99.9 | | 99.9 |
| | | w/o Factors | 0.2 | 100.0 | | 100.0 | 0.5 | 100.0 | | 100.0 |
| 10% | Medium | MIMIX | 2.2 | 98.8 | 92.0 | 99.8 | 3.7 | 98.3 | 86.8 | 99.6 |
| | | w/o Factors | 2.8 | 98.6 | 76.4 | 100.0 | 3.9 | 98.7 | 68.6 | 100.0 |
| | High | MIMIX | 10.3 | 97.3 | 53.6 | 99.6 | 14.4 | 96.1 | 42.6 | 99.4 |
| | | w/o Factors | 14.6 | 96.5 | 24.8 | 100.0 | 17.9 | 96.0 | 18.6 | 100.0 |
| | Very High | MIMIX | 23.6 | 95.5 | 22.2 | 99.8 | 27.4 | 95.0 | 14.0 | 99.7 |
| | | w/o Factors | 28.9 | 93.9 | 6.2 | 100.0 | 31.7 | 93.5 | 2.2 | 100.0 |
| 20% | Medium | MIMIX | 3.9 | 98.0 | 94.0 | 99.4 | 6.3 | 96.7 | 85.7 | 99.0 |
| | | w/o Factors | 3.6 | 98.7 | 79.5 | 100.0 | 6.0 | 98.0 | 70.7 | 100.0 |
| | High | MIMIX | 16.2 | 95.6 | 58.9 | 99.4 | 20.3 | 94.5 | 54.6 | 99.3 |
| | | w/o Factors | 21.1 | 95.3 | 30.1 | 100.0 | 26.8 | 94.5 | 22.8 | 100.0 |
| | Very High | MIMIX | 36.1 | 93.0 | 26.7 | 99.5 | 41.7 | 91.7 | 18.7 | 99.6 |
| | | w/o Factors | 50.5 | 90.0 | 6.3 | 100.0 | 56.9 | 88.8 | 3.4 | 100.0 |

274 lower TPR at around 20% and 5% respectively, and greater difference in RMSE in favor of MIMIX.
275 Both methods are strongly conservative, achieving TNRs that are overwhelmingly 100%, and their
276 C95 is often greater than the expected 95%, except in extreme variance situations (very high error
277 variance, high block variance) with 20% dense fixed effects.

278 From the global and local simulation results, we draw three broad conclusions about the per-
279 formance of MIMIX, MIMIX w/o Factors, and PERMANOVA for microbiome data analysis in
280 designed experiments. First, at a global level, MIMIX and MIMIX w/o Factors achieve far greater
281 power and comparable type I error (about 0.05) to PERMANOVA. Moreover, the global tests for all
282 three methods appear more adversely affected by higher overdispersion in taxa counts than higher
283 variability introduced by blocking factors in the experimental design. Second, at the local level,
284 MIMIX is better suited for both the detection and estimation of sparse treatment effects compared
285 to MIMIX w/o Factors. In this case, MIMIX w/o Factors achieves lower TPR and higher RMSE
286 on average because it does not account for correlation patterns among taxa. Finally, TNR and C95

287 are very high and relatively consistent between the two methods under all simulation conditions,
288 suggesting MIMIX and MIMIX w/o Factors are conservative in detecting significant OTU-specific
289 fixed effects.

290 5 Analysis of the NutNet Experiment

291 We first compare the performance of MIMIX and MIMIX w/o Factors on the NutNet data through
292 five-fold cross-validation, setting the maximum number of latent factors (L) for MIMIX equal to
293 the number of samples (166). Specifically, for each \mathbf{Y}_i with total counts m_i we construct $\mathbf{Y}_i^{\text{test}f}$,
294 $f = 1, \dots, 5$ by assigning each of m_i observations to one of the five folds at random and let $\mathbf{Y}_i^{\text{train}f} =$
295 $\sum_{g \neq f} \mathbf{Y}_i^{\text{test}g}$. For each fold $f = 1, \dots, 5$, we fit both models to training data f , drawing 20,000
296 posterior samples and discarding the first 10,000 for burn-in. Next, we examine the difference of
297 their log-likelihoods (MIMIX minus MIMIX w/o Factors) evaluated on testing data f where the
298 multinomial probability vector is estimated by the normalized posterior mean vector of occurrence
299 probabilities $\hat{\phi}_i$. Over all five folds, 69% of differences are positive on average, favoring MIMIX.
300 Thus, MIMIX appears to be a more apt model for these data than MIMIX w/o Factors.

301 To assess whether MIMIX adequately captures the sparsity in the data, we fit a preliminary
302 model to the data and perform posterior predictive checks (Gelman et al., 2014). These checks
303 examine the proportion of OTUs within each sample with zero counts (sparsity). This is done by
304 predicting new $\mathbf{Y}_1, \dots, \mathbf{Y}_n$ from every posterior sample and comparing the sparsity and overdispersion
305 in these predicted samples with the observed data. With respect to sparsity, we also consider
306 the proportion of OTUs within each sample with two or fewer counts, as these singletons and dou-
307 bletons are thought by biologists to be generated by errors in the sequencing process. Figure 3
308 depicts posterior predictive checks on sparsity of MIMIX after 20,000 posterior samples with the first
309 10,000 removed for burn-in. MIMIX does not accurately estimate the proportion of OTUs within
310 each sample with exactly zero counts, but when singleton and doubleton counts are further consid-
311 ered the model recovers the observed near-sparsity of the original data. The distinction between zero

312 counts and two or fewer counts is likely of little consequence. Additional posterior predictive checks
 313 on the maximum proportion of total counts within a sample from a single OTU (overdispersion)
 314 and the average Bray-Curtis similarity between samples from the same site, block, and treatment
 315 group also suggest that the marginal and joint distributions of OTU counts are captured faithfully
 316 by the MIMIX fit (results in the Online Supplemental).

317 We now use MIMIX to characterize the effects of the nutrient-supplement and herbivore-exclusion
 318 treatments on the fungal foliar microbiome of *A. gerardii*. For the purposes of comparison, we also
 319 present analyses from Bray-Curtis PERMANOVA, which represents the current state-of-the-art in
 320 ecological analysis, and MIMIX w/o Factors. We present MIMIX w/o Factors to illustrate the con-
 321 sequences of using factor analysis to account for dependence patterns among taxa in the microbiome,
 322 but we emphasize that our simulation studies and preliminary analysis point towards MIMIX as
 323 the most trustworthy analysis. For the Bayesian models, we collect 20,000 posterior samples and
 324 discard the first 10,000 for burn-in.

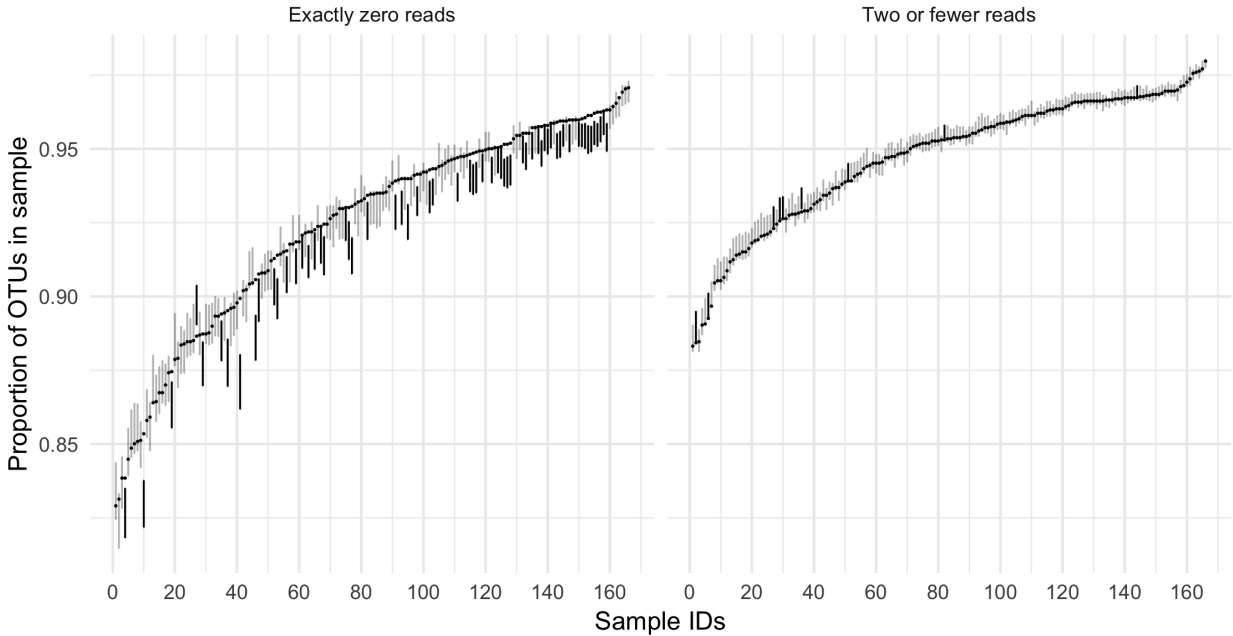


Figure 3: Posterior predictive checks on sparsity for MIMIX applied to the NutNet data. For each sample, the dot indicates the proportion of OTUs in the sample with 0 (left) or ≤ 2 (right) reads. The vertical line is the 95% posterior predictive distribution, shaded black if the interval excludes the observed value and gray otherwise.

325 First, we conduct a global test of whether the experimental treatments affect the overall com-
326 position of the microbiome. No method identifies a significant interaction effect between the two
327 treatments, with PERMANOVA $p = 0.120$, MIMIX posterior probability 0.236, and MIMIX w/o
328 Factors posterior probability 0.413. However, PERMANOVA and MIMIX find strong evidence that
329 the fungal microbiome composition is affected by nutrient supplement, with $p = 0.003$ and posterior
330 probability 1.0, respectively, while MIMIX w/o Factors does not, with posterior probability 0.757.
331 No method detects an effect of herbivore exclusion, with PERMANOVA $p = 0.787$, MIMIX poste-
332 rior probability 0.196, and MIMIX w/o Factors posterior probability 0.523. These results suggest
333 that the composition of the foliar fungal microbiome of *A. gerardii* is impacted by the resources
334 available to the plant host.

335 We next use MIMIX to estimate the effects of nutrient supplement on individual fungal OTUs.
336 Because the OTU assignments for this particular data set are only preliminary, we focus here on the
337 distribution of OTU-level effects, and reserve the characterization of effects on specific OTUs for
338 later work. The fixed effect for nutrient supplement estimated by MIMIX has 95% credible intervals
339 that exclude zero for 73 OTUs (Figure 4). Thus, while this analysis finds overwhelming evidence
340 that environmental nutrient supply alters the composition of these microbiomes, this effect appears
341 to be driven by only a few constituent microbes. Moreover, it appears accounting for correlation
342 among OTUs is essential to detecting these individual microbes. In the Online Supplement, we show
343 that estimates of OTU-level treatment effects are robust to the choice of variance hyperparameters
344 c_0 and d_0 .

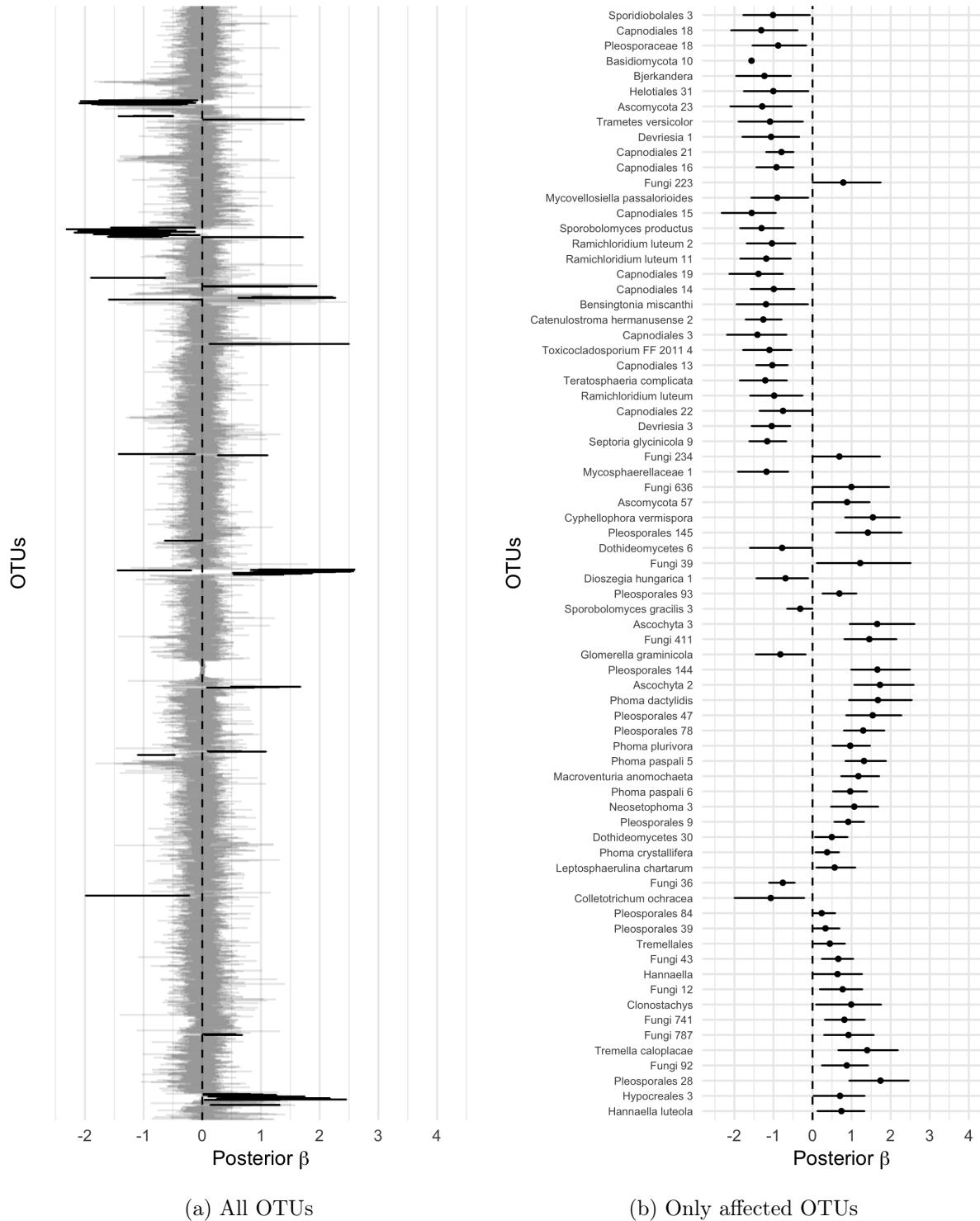


Figure 4: Posterior 95% credible intervals for the effect of nutrient supplement on each OTU. Across all OTUs (a), most are not significantly affected by the treatment (gray lines), but MIMIX identifies 73 of 2,662 OTUs (2.7%) that show a significant response (black lines). Among these affected OTUs (b), the taxonomy of each fungal OTU is given up to species, if known, or at a higher taxonomic rank, such as genus or order, with trailing numbers identifying distinct strains. The OTUs are ordered along the y-axis according to complete linkage hierarchical clustering of the estimated factor correlation matrix from MIMIX.

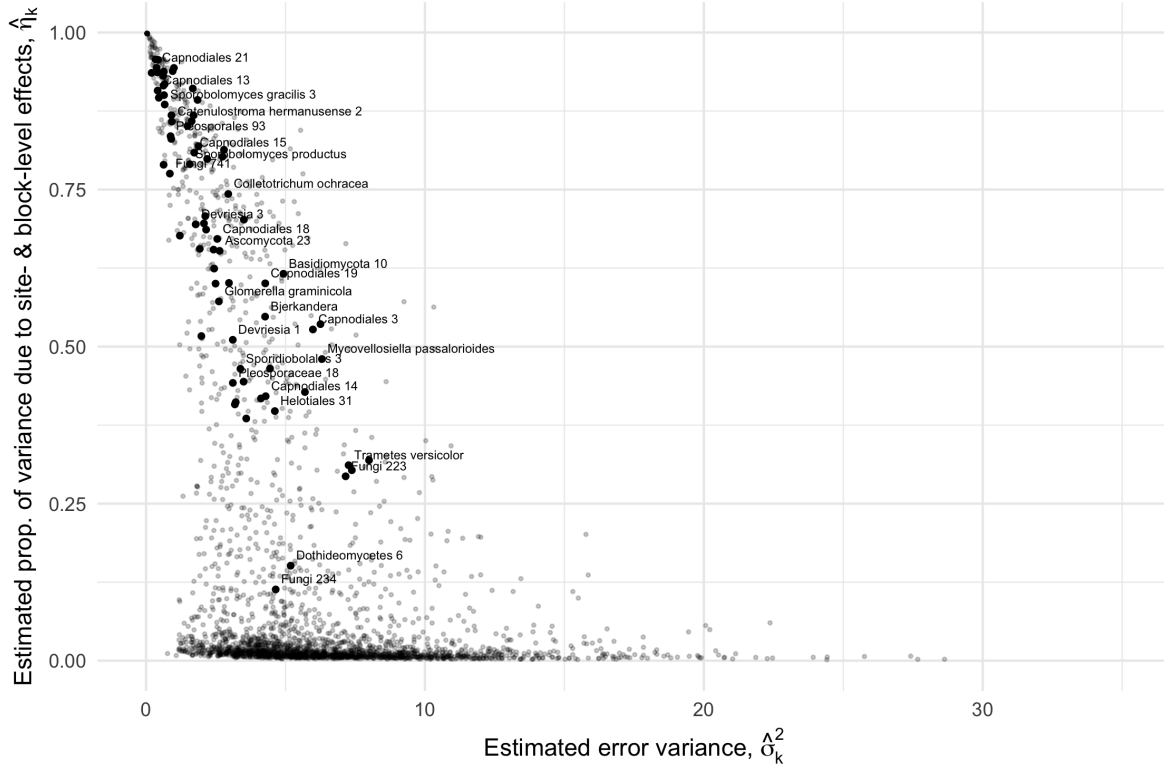


Figure 5: The proportion of variance for each OTU that is explained by the contribution of site and block vs. unexplained residual variation. Black dots correspond to OTUs identified by MIMIX as being significantly affected by nutrient supplement in Figure 4b, though only a subset of names are displayed to avoid overlapping labels.

345 MIMIX quantifies the relative contribution of different sources of residual variation to fungal
 346 composition. Site- and block-level variances are estimated with posterior means $\hat{\sigma}_{\text{Site}}^2 = 3.279$ and
 347 $\hat{\sigma}_{\text{Block}}^2 = 0.296$. Posterior means of OTU-specific variances not attributed to the study design
 348 $(\hat{\sigma}_1^2, \dots, \hat{\sigma}_K^2)$ are strongly skewed, ranging from 0.032 to 28.63 with mean 5.817 (Figure 5). The
 349 proportion of residual variance in OTU k that is captured by site- and block-level effects is estimated
 350 by

$$351 \quad \hat{\eta}_k = 1 - \frac{\hat{\sigma}_k^2}{\hat{\sigma}_k^2 + (1 + \hat{\sigma}_{\text{Site}}^2 + \hat{\sigma}_{\text{Block}}^2) \sum_{l=1}^L \hat{\lambda}_{lk}^2},$$

352 where $\hat{\lambda}_{lk}$ is the posterior mean of λ_{lk} . Figure 5 shows $\hat{\eta}_k$ vs. $\hat{\sigma}_k^2$ for each OTU.

353 Two loose groups of points emerge, one in which residual variation is almost entirely explained by
 354 site and block variation ($\hat{\eta}_k > 0.4$), and another in which these random effects explain a relatively
 355 small amount of residual variation in OTUs ($\hat{\eta}_k < 0.4$). OTUs identified by MIMIX as being

356 significantly affected by nutrient supplement, indicated by black dots in Figure 5, appear to be
 357 strongly represented in the former of these two groups, although there are a few OTUs that are
 358 significantly affected by nutrient supplement that do not appear to be greatly influenced by site and
 359 block effects. Overall, site and block effects explain over half the residual variation ($\hat{\eta}_k > 0.5$) for

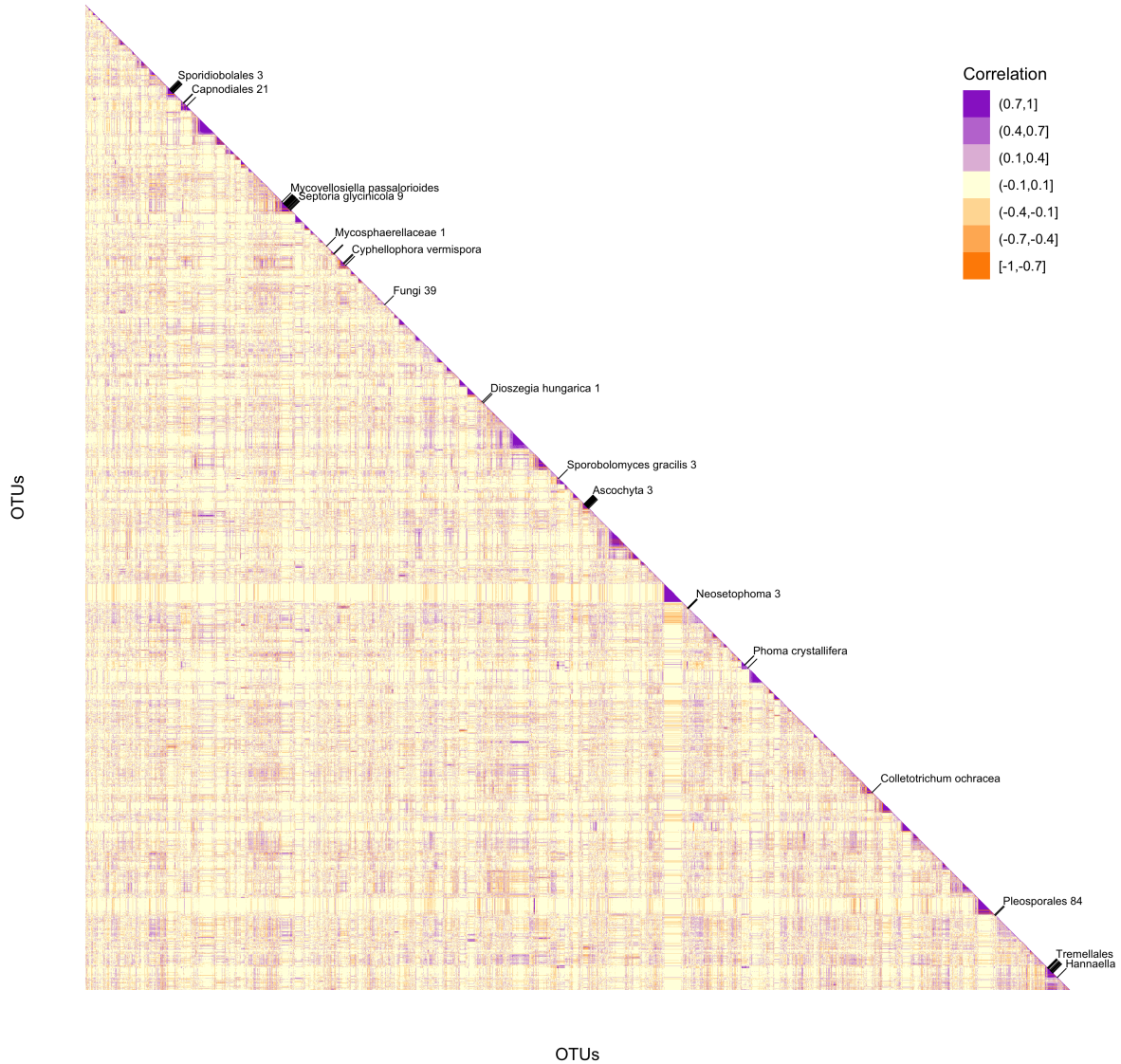


Figure 6: Estimated factor correlation matrix among OTUs, with OTUs ordered by hierarchical clustering. Clusters of strongly correlated OTUs, represented by purple triangles along the diagonal, indicate small communities that respond similarly to the fixed and random effects of the designed experiment. The OTUs highlighted along the diagonal are those identified by MIMIX as being significantly affected by nutrient supplement in Figure 4b, though only a subset of names are displayed to avoid overlapping labels.

360 approximately 16% of OTUs.

361 Finally, we take a closer look at the estimated factor correlation matrix $\mathbf{\Lambda}\mathbf{\Lambda}'$ using the posterior
362 mean of $\mathbf{\Lambda}$ (Figure 6). MIMIX identifies a large number of potential clusters of fungal OTUs
363 (grouped along the diagonal of Figure 6), with myriad positive and negative correlations among
364 them. These clusters may indicate latent ecological subcommunities, or they may reflect collections
365 of taxa that occupy similar ecological niches. MIMIX w/o Factors does not adequately account for
366 these relationships among OTUs, which explains its poorer fit to the data.

367 6 Discussion

368 In this paper, we introduce MIMIX (Microbiome MIXed effects), a Bayesian mixed-effects model
369 to analyze microbiome data as a response variable in designed experiments. MIMIX has several
370 attractive features for the analysis of high-dimensional, sparse, microbiome count data. It performs
371 spike-and-slab variable selection to identify treatment effects on individual Operational Taxonomic
372 Units (OTUs). Moreover, its Bayesian factor analysis formulation with a continuous shrinkage
373 Dirichlet-Laplace prior clusters OTUs into different factors based on how they respond to the fixed
374 and random effects in the experiment. This allows for post-hoc analysis of the model to identify be-
375 haviorally similar clusters of OTUs within the larger microbiome community. In a simulation study,
376 these features allow MIMIX to outperform both PERMANOVA with Bray-Curtis dissimilarity and
377 MIMIX that does not include Bayesian factors (MIMIX w/o Factors) in identifying and estimating
378 sparse treatment effects.

379 We demonstrate MIMIX on experimental data from four sites within the Nutrient Network
380 cooperative to quantify the effects of nutrient supplement and herbivore exclusion on the fungal
381 microbiome of the grass species *Andropogon gerardii*. We identify a significant effect of nutrient
382 supplement (but not herbivore exclusion) on these microbiomes, while accounting for random effects
383 due to both site and blocks within site. We also identify a significant treatment effect of nutrient
384 supplement on about 2.7% of OTUs. Although the OTU assignments in this particular data set

385 are preliminary, our results illustrate how MIMIX enables OTU-level inferences that may allow
386 for deeper and sharper understanding of how environmental conditions impact the abundance of
387 specific taxa in a microbiome.

388 Ecologically, this analysis of the Nutrient Network data suggests the following insights. First,
389 ecologists are frequently interested in how resource supply and grazing combine to influence the
390 structure of ecological communities (the so-called “bottom-up” vs. “top-down” dichotomy). The
391 results of this experiment suggest that resource supply, or “bottom-up” factors, play a larger role in
392 structuring a host’s microbiome than predation. Second, the paucity of large OTU-specific responses
393 (Figure 4) suggests that only a handful of microbial taxa respond to the nutrient supplementation,
394 and that these responses can be sufficient to reshape the microbiome when considered as an ecological
395 whole. Third, the residual variation of some, though not all OTUs can be explained by site- and
396 block-level random effects (Figure 5), suggesting that these OTUs may either be strongly influenced
397 by regional environmental correlates, or may be limited by reduced dispersal at regional (km) scales.
398 Finally, the estimated factor correlation matrix (Figure 6) suggests that this foliar microbiome is
399 composed of many modestly sized clusters of similarly behaving OTUs. This pattern may either
400 suggest many moderately sized subcommunities, aggregation of taxa into many separate ecological
401 niches, or both.

402 The initial results from MIMIX are encouraging, but its features will need to scale as microbiome
403 experiments grow in complexity. For example, MIMIX is not currently suited for handling data
404 from longitudinal studies with repeated measures over time. Furthermore, while the dimensionality
405 of the microbiome data analyzed here is quite high at $K \approx 2,500$, the dimensionality can grow
406 rapidly, especially when multiple domains of life (bacteria, archaea, fungi, etc.) are studied. In
407 such instances, computation time and memory management will become a more pressing concern
408 which may require a reconstruction of the posterior sampling scheme. We set the number of latent
409 factors to be the maximum number of identifiable factors and allow the Bayesian shrinkage prior
410 to eliminate excess factors. Another approach that may be more suitable for massive datasets is to
411 use a smaller number of latent factors with Gaussian priors on the factor matrix. This approach is

412 easier to explain and implement, and faster for a given number of factors. However, this approach
413 would likely require expensive cross-validation to pick the number of factors and would not account
414 for uncertainty in the number of factors.

415 **Funding**

416 This work was supported by National Science Foundation award EF-1241794.

417 **References**

- 418 Aitchison, John (1986). *The statistical analysis of compositional data*. Chapman & Hall, London.
- 419 Alivisatos, A Paul, MJ Blaser, Eoin L Brodie, Miyoung Chun, Jeffrey L Dangl, Timothy J Donohue,
420 Pieter C Dorrestein, Jack A Gilbert, Jessica L Green, Janet K Jansson, et al. (2015). “A unified
421 initiative to harness Earth’s microbiomes”. *Science* 350.6260, pages 507–508.
- 422 Bezanson, Jeff, Alan Edelman, Stefan Karpinski, and Viral B. Shah (2017). “Julia: A Fresh Approach
423 to Numerical Computing”. *SIAM Review* 59.1, pages 65–98.
- 424 Bhattacharya, Anirban, Debdeep Pati, Natesh S Pillai, and David B Dunson (2015). “Dirichlet–
425 Laplace priors for optimal shrinkage”. *Journal of the American Statistical Association* 110.512,
426 pages 1479–1490.
- 427 Billheimer, Dean, Peter Guttorp, and William F Fagan (2001). “Statistical interpretation of species
428 composition”. *Journal of the American statistical Association* 96.456, pages 1205–1214.
- 429 Bond-Lamberty, Ben, Harvey Bolton, Sarah Fansler, Alejandro Heredia-Langner, Chongxuan Liu,
430 Lee Ann McCue, Jeffrey Smith, and Vanessa Bailey (2016). “Soil respiration and bacterial struc-
431 ture and function after 17 years of a reciprocal soil transplant experiment”. *PloS one* 11.3,
432 e0150599.
- 433 Borer, Elizabeth T, W Stanley Harpole, Peter B Adler, Eric M Lind, John L Orrock, Eric W
434 Seabloom, and Melinda D Smith (2014). “Finding generality in ecology: a model for globally
435 distributed experiments”. *Methods in Ecology and Evolution* 5.1, pages 65–73.

436 Bray, J Roger and John T Curtis (1957). “An ordination of the upland forest communities of
437 southern Wisconsin”. *Ecological monographs* 27.4, pages 325–349.

438 Carvalho, Carlos M, Jeffrey Chang, Joseph E Lucas, Joseph R Nevins, Quanli Wang, and Mike West
439 (2008). “High-dimensional sparse factor modeling: Applications in gene expression genomics”.
440 *Journal of the American Statistical Association* 103.484, pages 1438–1456.

441 Chen, Eric and Hongzhe Li (2016). “A two-part mixed-effects model for analyzing longitudinal
442 microbiome compositional data”. *Bioinformatics*, btw308.

443 Chen, Jun and Hongzhe Li (2013). “Variable selection for sparse Dirichlet-multinomial regression
444 with an application to microbiome data analysis”. *The annals of applied statistics* 7.1.

445 Gelman, Andrew, John B Carlin, Hal S Stern, and Donald B Rubin (2014). *Bayesian data analysis*.
446 Volume 2. Chapman & Hall/CRC Boca Raton, FL, USA.

447 Grantham, Neal S, Brian J Reich, Krishna Pacifici, Eric B Laber, Holly L Menninger, Jessica B
448 Henley, Albert Barberán, Jonathan W Leff, Noah Fierer, and Robert R Dunn (2015). “Fungi
449 identify the geographic origin of dust samples”. *PloS one* 10.4, e0122605.

450 La Rosa, Patricio S, J Paul Brooks, Elena Deych, Edward L Boone, David J Edwards, Qin Wang,
451 Erica Sodergren, George Weinstock, and William D Shannon (2012). “Hypothesis testing and
452 power calculations for taxonomic-based human microbiome data”. *PloS one* 7.12, e52078.

453 Lozupone, Catherine and Rob Knight (2005). “UniFrac: a new phylogenetic method for comparing
454 microbial communities”. *Applied and environmental microbiology* 71.12, pages 8228–8235.

455 McArdle, Brian H and Marti J Anderson (2001). “Fitting multivariate models to community data:
456 a comment on distance-based redundancy analysis”. *Ecology* 82.1, pages 290–297.

457 McMurdie, Paul and Susan Holmes (2014). “Waste not, want not: why rarefying microbiome data
458 is inadmissible”. *PLoS Comput Biol* 10.4, e1003531.

459 Metzker, Michael L (2010). “Sequencing technologies —the next generation”. *Nature reviews genetics*
460 11.1, pages 31–46.

461 Mitchell, Toby J and John J Beauchamp (1988). “Bayesian variable selection in linear regression”.
462 *Journal of the American Statistical Association* 83.404, pages 1023–1032.

463 Neal, Radford M et al. (2011). “MCMC using Hamiltonian dynamics”. *Handbook of Markov Chain*
464 *Monte Carlo* 2, pages 113–162.

465 Pearson, Karl (1896). “Mathematical contributions to the theory of evolution.—On a form of spurious
466 correlation which may arise when indices are used in the measurement of organs”. *Proceedings*
467 *of the Royal Society of London* 60.359-367, pages 489–498.

468 Ren, Boyu, Sergio Bacallado, Stefano Favaro, Susan Holmes, and Lorenzo Trippa (2017). “Bayesian
469 nonparametric ordination for the analysis of microbial communities”. *Journal of the American*
470 *Statistical Association* 112.520, pages 1430–1442.

471 Rowe, Daniel B (2002). *Multivariate Bayesian statistics: models for source separation and signal*
472 *unmixing*. CRC Press.

473 Shafiei, Mahdi, Katherine A Dunn, Eva Boon, Shelley M MacDonald, David A Walsh, Hong Gu, and
474 Joseph P Bielawski (2015). “BioMiCo: a supervised Bayesian model for inference of microbial
475 community structure”. *Microbiome* 3.1, page 8.

476 Wadsworth, W Duncan, Raffaele Argiento, Michele Guindani, Jessica Galloway-Pena, Samuel A
477 Shelburne, and Marina Vannucci (2017). “An integrative Bayesian Dirichlet-multinomial regres-
478 sion model for the analysis of taxonomic abundances in microbiome data”. *BMC Bioinformatics*
479 18.1, page 94.

480 Warton, David I, Stephen T Wright, and Yi Wang (2012). “Distance-based multivariate analyses
481 confound location and dispersion effects”. *Methods in Ecology and Evolution* 3.1, pages 89–101.

482 Wu, Gary D and James D Lewis (2013). “Analysis of the human gut microbiome and association
483 with disease”. *Clinical gastroenterology and hepatology: the official clinical practice journal of the*
484 *American Gastroenterological Association* 11.7.

485 Xia, Fan, Jun Chen, Wing Kam Fung, and Hongzhe Li (2013). “A logistic normal multinomial
486 regression model for microbiome compositional data analysis”. *Biometrics* 69.4, pages 1053–
487 1063.

488 Zhang, Xinyan, Himel Mallick, Zaixiang Tang, Lei Zhang, Xiangqin Cui, Andrew K Benson, and
489 Nengjun Yi (2017). “Negative binomial mixed models for analyzing microbiome count data”.
490 *BMC Bioinformatics* 18.1, page 4.